

Flow manipulation around the Ahmed body with a rear window using passive strategies

Charles-Henri Bruneau^a, Patrick Gilliéron^b, Iraj Mortazavi^{a,*}

^a Université Bordeaux 1, CNRS UMR 5466, INRIA FUTURS équipe MC2, 351, cours de la Libération, 33405 Talence, France

^b Technocentre Renault, direction de la recherche, groupe mécanique des fluides et aérodynamique,
1, avenue du Golf, 78288 Guyancourt cedex, France

Received 23 February 2007; accepted 13 March 2007

Presented by Michel Combaroum

Abstract

The control of two-dimensional flows around the Ahmed body with a rear window on top of a road is achieved using porous devices added on some parts of the body. The modelling of the flow in different media is performed by means of the penalisation method. A good choice of the location of the porous interfaces yields an improvement of the aerodynamic parameters. *To cite this article: C.-H. Bruneau et al., C. R. Mecanique 335 (2007).*

© 2007 Académie des sciences. Published by Elsevier Masson SAS. All rights reserved.

Résumé

Manipulation passive d'écoulements autour du corps d'Ahmed à lunette arrière. Une méthode de contrôle passif utilisant une interface poreuse est appliquée à l'écoulement du corps d'Ahmed à lunette arrière sur une route en dimension deux. L'écoulement à l'intérieur des différents milieux est modélisé par une méthode de pénalisation. Les résultats montrent qu'un choix approprié des milieux poreux conduit à des gains au niveau des paramètres aérodynamiques. *Pour citer cet article : C.-H. Bruneau et al., C. R. Mecanique 335 (2007).*

© 2007 Académie des sciences. Published by Elsevier Masson SAS. All rights reserved.

Keywords: Computational fluid mechanics; Ahmed body; Porous interface

Mots-clés : Mécanique des fluides numérique ; Corps d'Ahmed ; Interface poreuse

Version française abrégée

La réduction de traînée des véhicules automobiles constitue aujourd’hui un enjeu majeur pour réduire la consommation et donc les émissions de gaz à effet de serre. Dans ce contexte, les constructeurs recherchent des solutions innovantes capables de réduire de 30% la traînée aérodynamique des véhicules automobiles sans contraindre le design,

* Corresponding author.

E-mail addresses: bruneau@math.u-bordeaux1.fr (C.-H. Bruneau), patrick.gillieron@renault.com (P. Gilliéron), mortaz@math.u-bordeaux1.fr (I. Mortazavi).

le confort, l'habitabilité et la sécurité des occupants. Les solutions s'obtiennent par contrôle pariétal des écoulements et des décollements à l'aide de dispositifs actifs ou passifs [1]. Parmi ces solutions, l'utilisation de systèmes passifs reste privilégiée pour des raisons évidentes de coût et des résultats significatifs peuvent être obtenus à partir de techniques simples à mettre en œuvre [2]. Parmi ces techniques, l'utilisation de surfaces poreuses peut constituer une voie de progrès intéressante [3]. Des milieux poreux distribués sur la surface des véhicules peuvent en effet permettre de réduire les déficits pariétaux de vitesse, de reporter vers l'aval la position des décollements, de réduire les dimensions transversales des sillages, le développement des structures tourbillonnaires longitudinales et donc la traînée aérodynamique. Dans cette perspective, des recherches sont effectuées à partir d'expérimentations numériques pour identifier les paramètres d'influence ainsi qu'analyser et quantifier l'impact de cette solution sur la traînée aérodynamique. Dans ce travail, la simulation numérique s'effectue sans modèle de turbulence à l'aide d'une méthode dite de pénalisation qui permet de résoudre simultanément les écoulements dans les milieux fluide et poreux. L'approche consiste à introduire un terme de pénalisation U/K dans les équations de Navier-Stokes où U et K représentent respectivement la vitesse et un coefficient sans dimension permettant de simuler la perméabilité des milieux fluide et poreux [3]. Les expérimentations numériques sont réalisées sur une représentation bidimensionnelle simplifiée de véhicule automobile désignée «corps de Ahmed» [4]. Les milieux poreux sont distribués sur les parties avant, haute et basse de la maquette qui représentent respectivement la face avant, le pavillon et le soubassement d'un véhicule automobile simplifié. Leur efficacité est alors analysée à partir de la valeur RMS du coefficient de portance, de l'enstrophie, des coefficients moyens de pression statique relevés au culot et des contributions avant, arrière et globale à la réduction de la traînée aérodynamique. Les résultats montrent que des réductions de traînée proches de 20% s'obtiennent pour des milieux poreux distribués sur les parties haute et basse de la géométrie. Ces réductions de traînée s'associent à de fortes valeurs des coefficients pariétaux de pression statique. L'importance des contributions des surfaces à faible rayon de courbure dans le développement des dimensions transversales de sillage et sur la traînée est d'autre part clairement mise en évidence. Cette contribution réduite aux surfaces de raccordement entre la face avant et les parties haute et basse de la géométrie est proche de 10%. L'influence d'un milieu poreux distribué sur l'avant apparaît d'autre part négligeable. Les résultats obtenus dans le cadre de ce travail confirment l'intérêt des milieux poreux pour mettre au point des solutions capables de réduire de manière significative la traînée aérodynamique des véhicules terrestres. Des expérimentations doivent cependant être poursuivies avec les ingénieurs de l'automobile sur des géométries 3D à complexité croissante pour tester l'efficacité de tels systèmes dans des environnements hostiles (pluie, boues, neige, ...) et identifier leur efficacité et capacité d'intégration sur véhicule.

1. Introduction

A simplified car, such as the Ahmed body [4], is a three-dimensional bluff body, moving in the vicinity of the ground, generating a turbulent flow. Several separations appear along the body from the front to the back. The resulting recirculation zones contribute to a significant part of the drag coefficient [5,6]. So, an objective of the control is to reduce the transverse separation area in the wake. The drag coefficient changes strongly with the angle α between the horizontal line and the rear window. The very well-known case in the literature, $\alpha = 25^\circ$, is studied in two dimensions to allow a wide range of low cost numerical tests in order to identify the main trends of the control. In this Note, passive control is achieved using porous interfaces to modify the boundary layer behaviour, and, consequently, to move downstream the separation line, to reduce the pressure gradients in the near wake and therefore the aerodynamic drag. A porous medium layer is inserted between the flow and the body to change the stress forces; indeed the no-slip boundary condition on the body surface is replaced by a mixed Fourier boundary condition on the walls [7,8]. Numerical studies have shown that significant reductions of the drag coefficient around a square cylinder or of the vortex induced vibrations on a riser pipe can be obtained [3,9]. The practical difficulty (to compute the flow in two different media, namely the fluid and the porous medium, with two models) is overcome using the penalisation method that allows one to solve simultaneously both flows with the same model. This method introduced in [10] is studied and validated in [11,12], applied to turbulent flows in [13] and to flow control in [3]; it consists in adding a penalisation term U/K in the incompressible Navier-Stokes equations where U is the velocity vector and K the non-dimensional permeability coefficient. This method can also be used as an immersed boundary method to avoid a body fitting and to solve directly the flow around bluff bodies on Cartesian meshes. In summary, we can solve the flow inside the three different media only by changing the value of the parameter K in the penalised Navier-Stokes equations.

In the following we describe the penalised Navier–Stokes equations or Brinkman–Navier–Stokes equations and give a brief outline of the numerical approximation. Then we give various results of the original flow or the controlled flow around the Ahmed body on top of a road. We analyse these results and quantify the efficiency of the passive control using a porous layer.

2. Numerical simulation

The penalised non-dimensional Navier–Stokes equations or Brinkman–Navier–Stokes equations for the non-dimensional unknowns (U, p) are

$$\partial_t U + (U \cdot \nabla) U - \frac{1}{Re} \Delta U + \frac{U}{K} + \nabla p = 0 \quad \text{in } \Omega_T = \Omega \times (0, T) \quad (1)$$

$$\operatorname{div} U = 0 \quad \text{in } \Omega_T \quad (2)$$

where $U = (u, v)$ is the velocity, p is the pressure, $K = \rho k \phi \bar{U} / \mu H$ is the non-dimensional coefficient of permeability of the medium (with k the intrinsic permeability, μ the viscosity, ϕ the porosity of the porous material, ρ the density of the fluid and H the height of the body) and Re is the Reynolds number. Finally, Ω is the full domain including the porous layer and the solid body. For more details on the numerical model the reader can refer to [3].

This model is able to represent the three media as follows. In the fluid the permeability coefficient goes to infinity, the penalisation term vanishes and we solve the non-dimensional Navier–Stokes equations. In the solid body the permeability coefficient goes to zero and it has been shown in [11] that solving these equations corresponds to solving Darcy's law in the solid and that the velocity is proportional to K . In the porous medium Brinkman equations are recovered. For numerical simulations we set $K = 10^{16}$ in the fluid and $K = 10^{-8}$ in the solid body; the porous medium is represented by $K = 10^{-1}$ that represents a high porosity and permeability medium [3]. The numerical simulation is performed by solving Eqs. (1), (2) where K is set at the velocity points according to the medium they belong to. Adding a porous layer between the solid body and the fluid induces a reduction of the shear effects in the boundary layer and thus allows to control the flow. In addition as the pressure is computed inside the solid body, we can compute the drag and lift forces by integrating the penalisation term on the volume of the body [7]:

$$F_D = \int_{\text{body}} u/K \, dx; \quad F_L = \int_{\text{body}} v/K \, dx$$

where the body includes the porous layers. To quantify the effect of the control we shall compare the following quantities, the static pressure coefficient, the drag coefficient, the root mean-square of the lift coefficient and the enstrophy given by

$$C_p = 2(p - p_0)/(\rho|U|^2); \quad C_D = 2F_D/H; \quad C_L = 2F_L/H$$

$$C_{L\text{rms}} = \sqrt{1/T \int_0^T C_L \, dt}; \quad Z = 1/2 \int_{\Omega} |\omega|^2 \, dx$$

where p_0 is the inlet static pressure and $\omega = \partial_{x1}v - \partial_{x2}u$ is the scalar vorticity in 2D. Let us note that the static pressure is set to zero at the downstream section of the domain.

The unsteady equations (1), (2) are associated to an initial datum at time $t = 0$

$$U(x, 0) = U_0(x) \quad \text{in } \Omega$$

and the following boundary conditions (Fig. 1)

$$U = (1, 0) \quad \text{on } \Gamma_D, \quad U = (1, 0) \quad \text{on } \Gamma_0$$

and

$$\sigma(U, p)n + \frac{1}{2}(U \cdot n)^-(U - U_{\text{ref}}) = \sigma(U_{\text{ref}}, p_{\text{ref}})n \quad \text{on } \Gamma_N$$

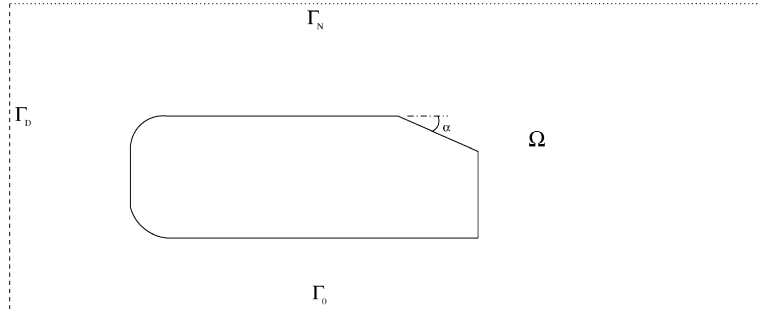


Fig. 1. Computational domain including the Ahmed body with a rear window.

where σ is the stress tensor and we use the notation $a = a^+ - a^-$. The far field boundary condition is used to convey the vortices through the artificial frontiers without any reflexion (see [14] for more details). Fig. 1 shows the computational domain.

The time discretization is achieved by means of the second-order Gear scheme with explicit treatment of the convection term. The space discretization uses a second-order centred scheme for all the linear terms and a third-order upwind scheme for convection terms [15]. The efficiency of the resolution is obtained by a multigrid procedure using a cell-by-cell relaxation smoother.

The non-dimensioned length and height of Ahmed body are respectively $L = 3.625$ and $H = 1$. The computational domain is $\Omega = (0.12H) \times (0.5H)$ and the body is located at a non-dimensioned distance $l = 1$ from the road. The results are presented on a 1536×640 cells uniform mesh in order to have a significant number of points in the porous layer of thickness $h = 0.1H$ for numerical efficiency as shown in [3].

3. Numerical results and analysis of the passive control

To comment the numerical results, we plot the mean pressure fields and the global quantities such as the enstrophy Z , the drag C_D and the root mean-square of the lift coefficient $C_{L\text{rms}}$ that reveals the regularity and steadiness of the flow. Let us note that up drag refers to the drag due to the front part of the body and down drag refers to the drag at the back. This allows us to analyse more carefully the impact of the control. The numerical tests have been performed for the Reynolds number $Re_L = Re \times L = 30\,000$ based on the length of the Ahmed body to have a highly transitional flow that corresponds to the studies of the literature [5]. Previous convergence studies have shown that the grid convergence is achieved for such Reynolds number on the used grids [9]. To have a good representation of the solutions we take up to 13 points in the porous layers.

The numerical tests are performed on an Ahmed body with a rear window of angle $\alpha = 25^\circ$ on top of a road for cases 0 (no control) and control cases 1 to 6 shown on Fig. 2. Although it is well known that the flow is fully three-dimensional and that the role of the longitudinal vortices cannot be neglected, we want to check if the size of the recirculation zone on the axis of symmetry of the body and the global flow parameters can be reduced. The mean pressure fields are shown on Fig. 3. The physical quantities and the minimum pressure in the near wake are given on Tables 1 and 2. The up drag is higher on the two first cases than the no control case and lower for the other cases. This higher value of the up drag for the cases 1 and 2 is due to the existence of the porous corners. The case 3 is the only one with an increase of the down drag. This is due to the non-symmetric vortex shedding at the back that is increased by the upper porous layer. The almost symmetric case 4 becomes very beneficial and reduces significantly the drag coefficient. The efficiency of the symmetric layers is also observed between cases 5 and 6 where the drag reduction reaches 10%. The best case is case 4 that has a uniform and quasi symmetric distribution of the porous layers on the bottom and the roof of the body, reducing significantly the vortex shedding in the back. Globally there is no significative gain on the drag coefficient except for case 4 (-21%) as there is a reduction on both up and down parts of the body. Nevertheless, the best compromise for the decrease of the global quantities is the case 6 where the flow is sharply regularised and the drag is also slightly reduced.

The above results are also verified for average pressure coefficient fields for the no-controlled case 0 and three representative controlled test cases 3, 4 and 6 in Fig. 3. As observed, the lower back vortex is strengthened in the case 3 compared to the no-controlled case. But, when adding the lower porous interface to the body in cases 4 and 6,

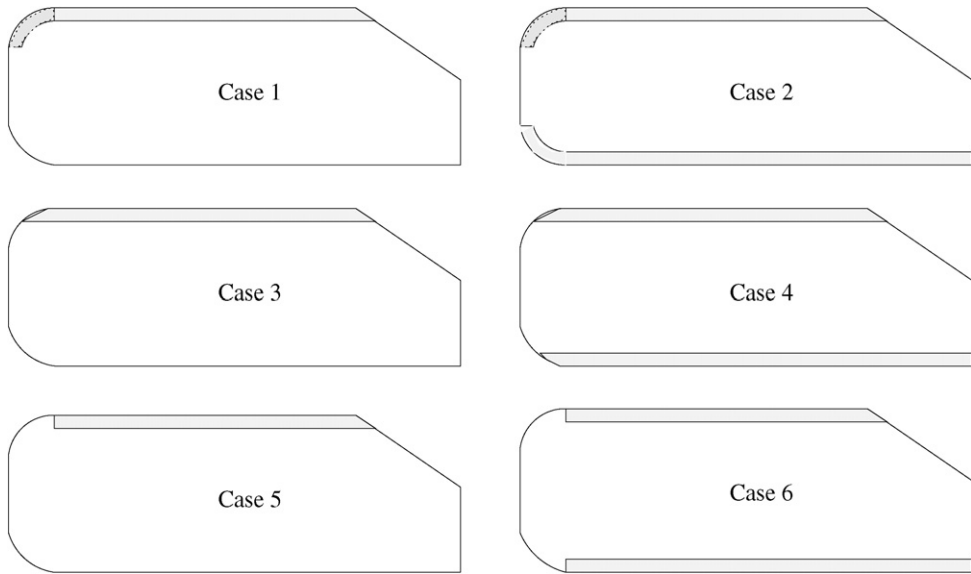


Fig. 2. Cases 1 to 6 corresponding to various porous device geometries.

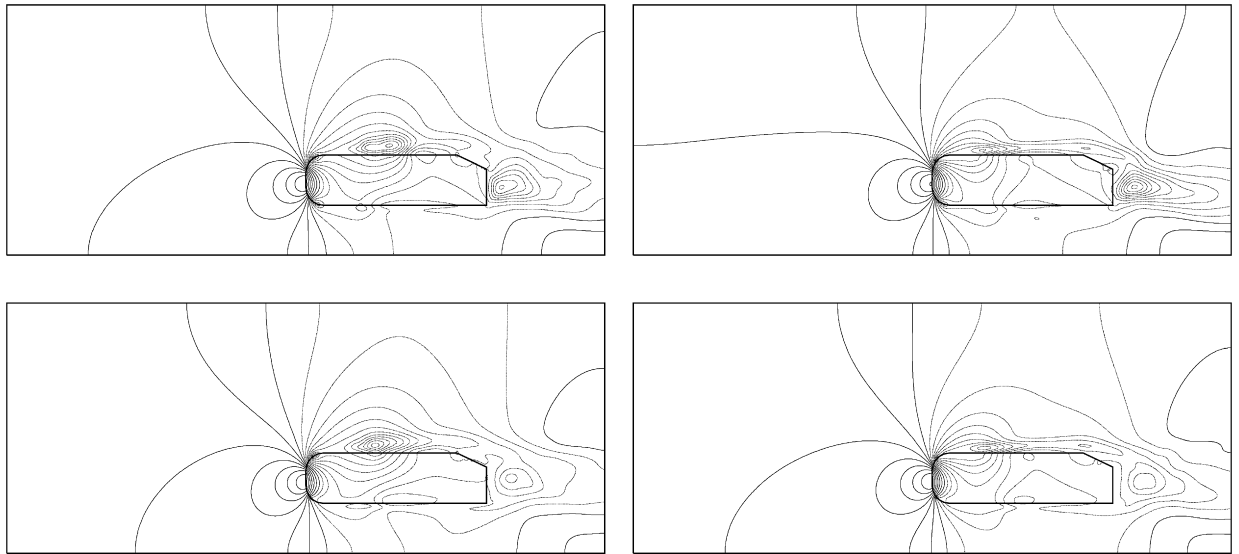
Fig. 3. Mean pressure isolines for the flow around Ahmed body with a rear window on top of a road at $Re_L = 30000$. Cases 0 (top left), 3 (top right), 4 (bottom left) and 6 (bottom right).

Table 1

Asymptotic values of $C_{L\text{rms}}$ and mean values of the enstrophy and the drag coefficient for Ahmed body with a rear window on top of a road at $Re_L = 30000$

	$C_{L\text{rms}}$	Enstrophy	Up drag	Down drag	Drag coefficient
Case 0	0.817	726	0.099	0.176	0.282
Case 1	0.687 (-16%)	551 (-24%)	0.138	0.118	0.264 (-6%)
Case 2	0.715 (-12%)	519 (-29%)	0.182	0.087	0.276 (-2%)
Case 3	0.600 (-27%)	605 (-17%)	0.100	0.190	0.300 (+6%)
Case 4	0.801 (-2%)	670 (-18%)	0.093	0.124	0.224 (-21%)
Case 5	0.595 (-27%)	590 (-19%)	0.088	0.167	0.265 (-6%)
Case 6	0.534 (-35%)	552 (-24%)	0.092	0.151	0.254 (-10%)

Table 2

The value and the location of the minimum mean pressure in the close wake of Ahmed body with a rear window on top of a road at $Re_L = 30000$

	P_{\min} value in the wake	P_{\min} location
Case 0	−0.813	(9.92, 1.36)
Case 3	−1.021	(10.06, 1.36)
Case 4	−0.543	(10.13, 1.50)
Case 6	−0.574	(10.17, 1.41)

the back vorticity is reduced and the eddy is detached from the wall. This coincides with an increase of the back static pressure and therefore with a decrease of the drag forces. Table 2 with minimum pressure values confirms these observations. To obtain more significant gain it would be necessary to reattach the flow at the rear window as shown in previous studies of flow control [16,17].

4. Conclusion

A passive control technique using a porous slice implemented on some parts of the two-dimensional Ahmed body with a rear window on top of a road is tested to reduce global quantities such as the drag coefficient, the enstrophy or the $C_{L\text{rms}}$ of the flow.

The best drag reductions are obtained for straight and continuous porous sheaths placed both on bottom and roof regions. The front layers have no significant effect on the drag reduction.

This passive control approach is very promising as significant gains are obtained with a good choice of the layers location. Further work on coupling both passive and active control approaches will be performed on the three-dimensional Ahmed body to reattach the flow by a suction jet on the top of the rear window.

References

- [1] M. Gad-El Hak, Flow Control: Passive, Active and Reactive Flow Management, Cambridge Univ. Press, 2000.
- [2] P. Gilliéron, Contrôle des écoulements appliqués à l'automobile, état de l'art, Mécanique et Industries 3 (6) (2002).
- [3] C.-H. Bruneau, I. Mortazavi, Passive control of flow around a square cylinder using porous media, Int. J. Numer. Methods Fluids 46 (2004).
- [4] S.R. Ahmed, G. Ramm, G. Falting, Some salient features of the time averaged ground vehicle wake, SAE paper 840300, 1984.
- [5] P. Gilliéron, A. Spohn, Flow separations generated by a simplified geometry of an automotive vehicle, in: IUTAM Symp. Unsteady Separated Flows, 2002.
- [6] M. Onorato, A. Costelli, A. Garonne, Measurement through wake analysis, SAE Paper 569, 1984.
- [7] J.-P. Caltagirone, Sur l'interaction fluide–milieu poreux: Application au calcul des efforts exercés sur un obstacle par un fluide visqueux, C. R. Acad. Sci. Paris, Sér. II 318 (1994).
- [8] Y. Achdou, O. Pironneau, F. Valentin, Effective boundary conditions for laminar flows over periodic rough boundaries, J. Comp. Phys. 147 (1998).
- [9] C.-H. Bruneau, I. Mortazavi, Control of vortex shedding around a pipe section using a porous sheath, Int. J. Offshore Polar Engrg. 16 (2) (2006).
- [10] E. Arquis, J.P. Caltagirone, Sur les conditions hydrodynamiques au voisinage d'une interface milieu fluide–milieu poreux: application à la convection naturelle, C. R. Acad. Sci. Paris, Sér. II 299 (1984).
- [11] Ph. Angot, Ch.-H. Bruneau, P. Fabrie, A penalization method to take into account obstacles in incompressible viscous flows, Numer. Math. 81 (1999).
- [12] G. Carrou, Brinkmann model and double penalization method for the flow around a porous thin layer.
- [13] N. Kevlahan, J.M. Ghidaglia, Computation of turbulent flow past an array of cylinders using a spectral method with Brinkman penalization, Eur. J. Mech. B Fluids 20 (2001).
- [14] C.-H. Bruneau, P. Fabrie, Effective downstream boundary conditions for incompressible Navier–Stokes equations, Int. J. Numer. Methods Fluids 19 (1994).
- [15] C.-H. Bruneau, M. Saad, The 2d lid-driven cavity problem revisited, Computers & Fluids 35 (3) (2006).
- [16] P. Gilliéron, F. Chometon, Modelling of stationary three-dimensional detached airflows around an Ahmed Reference Body, in: ESAIM Proc. 7 (1999).
- [17] P. Gilliéron, Detailed analysis of the overtaking process, J. Mech. Engrg. 53 (2003).